植物生态学报 2021, **45** (4): 394-403
Chinese Journal of Plant Ecology
扫码提问
DOI: 10.17521/cjpe.2020.0367
http://www.plant-ecology.com

中亚热带喀斯特常绿落叶阔叶混交林典型树种的木质部解剖与功能特征分析

倪鸣源 ARITSARA Amy Ny Aina 王永强 黄冬柳 项 伟 万春燕 朱师丹*

广西大学亚热带农业生物资源保护与利用国家重点实验室, 南宁 530004; 广西大学林学院广西森林生态与保育重点实验室, 南宁 530004

摘 要 树木木质部主要由导管、纤维和薄壁组织组成, 分别具有运输、支撑和贮存的生理功能。由于木质部空间限制, 一种组织比例的增加会导致其他组织比例的降低, 因而可能表现出权衡关系。分析木质部组织比例和权衡关系有助于了解植物的生理生态适应性。该研究选择中亚热带喀斯特常绿落叶阔叶混交林21种典型树种(10种落叶树种, 11种常绿树种), 测定枝条木质部各组织比例, 计算水力相关指标并分析性状之间的相关性。结果表明: (1)与全球木质部解剖数据对比分析, 喀斯特树种木质部趋向具有较高比例的薄壁组织; (2)喀斯特树种导管组织比例与薄壁和纤维组织比例之间没有显著的相关性, 但是薄壁和纤维组织比例之间有显著的权衡关系; (3)常绿和落叶树种的木质部水力运输安全性(导管壁加固系数)和效率性(理论导水率)均具有显著的权衡关系, 但是这两个类群线性回归的截距存在显著差异, 即在相同的理论导水率条件下, 落叶树种比常绿树种具有较高的导管壁加固系数(安全性), 可能与常绿树种具有更多的轴向薄壁组织有关。喀斯特树种木质部解剖特征表明薄壁组织的贮存功能对喀斯特树种(尤其是常绿树种)的干旱适应具有重要作用。

关键词 导管组织; 薄壁组织; 纤维组织; 导管壁加固系数; 理论导水率; 权衡

倪鸣源, Aritsara ANA, 王永强, 黄冬柳, 项伟, 万春燕, 朱师丹 (2021). 中亚热带喀斯特常绿落叶阔叶混交林典型树种的木质部解剖与功能特征分析. 植物生态学报, 45, 394-403. DOI: 10.17521/cjpe.2020.0367

Analysis of xylem anatomy and function of representative tree species in a mixed evergreen and deciduous broad-leaved forest of mid-subtropical karst region

NI Ming-Yuan, ARITSARA Amy Ny Aina, WANG Yong-Qiang, HUANG Dong-Liu, XIANG Wei, WAN Chun-Yan, and ZHU Shi-Dan*

Guangxi Key Laboratory of Forest Ecology and Conservation, College of Forestry, Guangxi University, Nanning 530004, China; and State Key Laboratory for Conservation and Utilization of Subtropical Agro-bioresources, College of Forestry, Guangxi University, Nanning 530004, China

Abstract

Aims Vessel, fibers, and parenchyma are the main components of tree xylem. They are responsible for water transport, mechanical support, and water and nutrients storage. Given the limited xylem space, consistent investment in one type of tissue would constrain the space available for other types of tissue, thus resulting in a possible trade-off among different tissues in their fractions. Analysis of the fractions of tissue types in xylem and the trade-off would contribute to better understanding of the eco-physiological adaptation of plants.

Methods We selected 21 characteristic tree species (10 deciduous and 11 evergreen) from a mixed evergreen and deciduous broad-leaved forest located in the mid-subtropical karst region, and measured their xylem tissue fractions. In addition, we calculated the hydraulic-related structural traits in xylems and examined the correlations among various traits.

Important findings Compared to the global average values of xylem tissue fractions, the karst tree species tended to have a higher proportion of parenchyma. The fraction of vessel lumen was not correlated with fiber and parenchyma fractions across the tree species investigated. Instead, a significant trade-off was observed between fractions of fiber and parenchyma. A trade-off between the hydraulic efficiency (i.e. theoretical hydraulic conductivity) and safety (vessel wall reinforcement) was observed across both the deciduous and the evergreen tree species. The two contrasting group of karst trees differenced significantly in the intercepts of the lines for trade-offs. For

收稿日期Received: 2020-11-09 接受日期Accepted: 2021-01-18
基金项目: 广西八桂青年学者项目和广西自然科学基金(2017GXNSFBA198188)。Supported by the Guangxi Bagui Young Scholars Program and the Natural Science Foundation of Guangxi (2017GXNSFBA198188).
* 通信作者Corresponding author (zhushidan@gxu.edu.cn)

given conductivity, the deciduous tree species exhibited stronger vessel well reinforcement (safety) than the evergreen tree species, which might be due to the fact that evergreen trees species had more axial parenchyma. Hence, this study revealed the specificity of xylem anatomy in karst tree species. Water and resource storage in xylem parenchyma are vital to karst trees (evergreens in particular) for their adaptation to the water-limiting environment.

Key words vessel; parenchyma; fibers; vessel wall reinforcement coefficient; theoretical hydraulic conductivity; trade-off

Ni MY, Aritsara ANA, Wang YQ, Huang DL, Xiang W, Wan CY, Zhu SD (2021). Analysis of xylem anatomy and function of representative tree species in a mixed evergreen and deciduous broad-leaved forest of mid-subtropical karst region. *Chinese Journal of Plant Ecology,* 45, 394-403. DOI: 10.17521/cjpe.2020.0367

我国西南喀斯特是世界喀斯特连片分布面积最大的区域, 总面积超过55万km^2, 主要集中在广西、贵州和云南等省区(宋同清, 2015)。其中, 广西喀斯特分布面积达9.7万km^2, 喀斯特地貌富有特色(蒋忠诚等, 2007)。由于广西地处云贵高原的东南缘、南临北部湾, 受热带亚热带季风气候影响, 高温多雨, 岩溶作用强烈, 喀斯特地貌以峰丛洼地、峰丛谷地为主(袁道先, 1992)。与非喀斯特地区相比, 喀斯特环境具有岩石(碳酸盐岩)裸露程度高、土壤稀薄、水分下渗快等特点(袁道先, 1992; 陈洪松等, 2013)。喀斯特生态系统较为脆弱, 受长期人类活动影响, 植被退化严重; 其中广西喀斯特石漠化面积达2.37万km^2, 生态环境问题突出(胡宝清, 2014)。广西喀斯特地区的植物多样性高(宋同清, 2015), 为喀斯特石漠化地区的植被重建提供了丰富的"乡土恢复工具树种库", 因此亟需了解喀斯特植物的生理生态适应性(曹坤芳等, 2014)。

由于喀斯特生境的水分有效性低, 喀斯特森林植物具有明显的旱生性特点(彭晚霞等, 2008)。喀斯特植物的生理生态适应性, 尤其是水分生理研究受到广泛关注(Wang *et al*., 2018; Chen *et al*., 2019)。研究表明喀斯特树种可以通过较强的生理调整能力适应水分亏缺(Cao *et al*., 2020), 或通过发达的根系扩大水分来源(Geekiyanage *et al*., 2019)。前期基于中亚热带喀斯特地区的喀斯特木本植物脆弱性曲线分析发现喀斯特树种抗栓塞能力并不高于同区域的非喀斯特森林树种(Fan *et al*., 2011; 谭凤森等, 2019)。另外, 研究发现植物薄壁细胞比例高的其非结构性碳水化合物含量高(Plavcová *et al*., 2016; Pratt & Jacobsen, 2017), 可能高的薄壁细胞比例在抗旱性方面发挥作用(Tomasella *et al*., 2019)。因此研究喀斯特树木的木质部结构特征有助于理解喀斯特植物的干旱适应性。

木本植物木质部主要由导管(或管胞)、纤维和薄壁细胞组成, 各自执行不同的功能: 导管(或管胞)负责水分和无机离子的运输; 薄壁组织负责水和碳水化合物的储存; 纤维主要负责机械支持(Hacke & Sperry, 2001; Plavcová & Jansen, 2015; Morris *et al*., 2016b)。木质部不同组织相互联系, 形成有机整体, 为植物体正常有序的生理过程提供保障(周朝彬等, 2016)。由于木质部空间(横截面积)限制, 导管组织、纤维组织、薄壁细胞组织的比例存在权衡关系, 即分配给某一组织较多的空间, 会减少其他组织的可用空间(Pratt & Jacobsen, 2017)。木质部组织分配的最优化有助于木质部发挥其最大的功能(Carlquist, 2018), 体现了其对生存环境的适应(Godfrey *et al*., 2020)。

广西木论喀斯特位于西南喀斯特的核心区域, 保存有连片面积最大、原生性较强的喀斯特森林(刘璐等, 2012)。顶极群落类型为中亚热带常绿落叶阔叶混交林; 与同区域的非喀斯特森林相比, 落叶树种的比例较高。落叶与常绿植物的生理生态特征具有显著差异; 基于木质部结构方面的研究表明落叶植物具有较低的木材密度、较小的导管密度以及较大的导管直径(Choat *et al*., 2005)。本研究选取木论喀斯特常绿落叶阔叶混交林21种典型树种(包括11种常绿树种和10种落叶树种), 测定枝条木质部解剖结构并计算相关水力功能性状。主要研究以下3个问题: (1)与全球数据相比, 喀斯特树种木质部解剖结构特征有何特殊性? (2)喀斯特树种木质部各组分之间是否具有显著的权衡关系? (3)喀斯特落叶与常绿树种的木质部结构和水力特征有何差异?

1 材料和方法

1.1 地理概况

研究样地位于广西河池市环江毛南族自治县木

论国家级自然保护区的永久性监测样地(25.15° N, 108.04° E), 海拔420 m。受季风气候影响, 该样地年平均气温19.2 ℃, 年降水量1 529.2 mm; 雨季为4–8月, 降水量占全年的73.7% (刘璐等, 2012)。森林群落类型为中亚热带喀斯特常绿落叶阔叶混交林, 样地面积为1 hm^2 (100 m × 100 m), 东南向; 处于喀斯特峰丛洼地中上坡, 平均坡度约27°, 岩石裸露率80%–90% (郑颖吾, 1999)。样地共有物种44科73属95种; 重要值靠前的树种为青檀(*Pteroceltis tatarinowii*)、广西密花树(*Myrsine kwangsiensis*)、千里香(*Murraya paniculata*)和菜豆树(*Radermachera sinica*)等。土壤以石灰土为主, 有机碳含量为15–24 $g \cdot kg^{-1}$ (刘淑娟等, 2010; 宋同清, 2015)。

1.2 实验材料

取样时间为2019年8月, 选取样地中21种典型的喀斯特木本植物, 隶属于14科21属, 其中落叶10种, 常绿11种(表1)。根据树种的平均树高与胸径, 每种选取5株健康成熟个体, 从每个个体上剪取2段冠层阳生枝条, 长度5 cm, 直径为7–10 mm。

1.3 测定方法

将采回的新鲜枝条放入贴好标签的离心管中, 用FAA溶液固定一周后, 将样品固定在滑走切片机(Leica SM2010R, Leica, Nusslock, Germany)的凹槽进行横切, 切片厚度为25 μm, 用乙酸乙酯溶解泡沫(聚苯乙烯)的混合液涂抹样品切面防止切片变形(Barbosa *et al*., 2010), 用鸡蛋清和甘油的混合液把切片粘在载玻片上, 再用番红溶液和阿利新蓝溶液染色, 依次经过浓度为40%、70%、90%、100%的酒精脱水后用加拿大树胶固定。利用光学显微镜(Leica DM 3000, Leica, Wetzlar, Germany)观察并对木质部横切面(边材)进行拍照。每个个体制作2个切片, 每个切片分别在10、20、40倍镜下随机拍摄4个视野。

利用ImageJ 1.52软件(www.imagej.nih.gov, USA; Rueden *et al*., 2016)对染色后的切片图(图1)进行分析处理, 得出以下指标: (1)导管密度(*Vd*), 即单位视野内的导管数量(Perez-Harguindeguy *et al*., 2013); (2)导管比例(*Vs*)、环管管胞比例(*Tr*)、导管壁比例、轴向薄壁组织比例(*APf*)、射线组织比例(*RPf*)以及纤维组织比例(*Fb*), 其中薄壁组织在次生木质部中是由射线细胞和轴向薄壁细胞两部分活细胞组成(Morris *et al*., 2016a); (3)相连接两个导管的细胞壁厚度之和(*t*)、相连接两个导管长短轴直径平均值(*b*)(Hacke *et al*., 2001)。其中, 导管壁的加固系数为导管壁厚度(*t*)与导管直径(*b*)的比值。导管壁加固系数与枝条的栓塞脆弱性有很强的相关性, *t*/*b*越大, 抗栓塞能力越强(Hacke *et al*., 2001)。同时, 根据木质部导管结构特征, 计算以下水力相关性状:

表1 广西木论21种喀斯特树种的叶习性、胸径和树高(平均值±标准差)
Table 1 Leaf types by longevity, diameter at breast-height (*DBH*), and height of the 21 karst tree species studied in Mulun, Guangxi (mean ± *SD*)

物种 Species	科 Family	胸径 *DBH* (cm)	树高 Height (m)
落叶 Deciduous			
黄梨木 *Boniodendron minus*	无患子科 Sapindaceae	12.4 ± 0.3	8.3 ± 0.2
禾串树 *Bridelia balansae*	大戟科 Euphorbiaceae	13.6 ± 1.0	7.5 ± 0.5
大叶紫珠 *Callicarpa macrophylla*	马鞭草科 Verbenaceae	6.5 ± 0.4	5.5 ± 0.7
麻楝 *Chukrasia tabularis*	楝科 Meliaceae	12.0 ± 1.4	8.0 ± 0.5
浆果楝 *Cipadessa baccifera*	楝科 Meliaceae	7.9 ± 1.1	6.4 ± 0.9
毛果巴豆 *Croton lachnocarpus*	大戟科 Euphorbiaceae	8.4 ± 0.3	6.5 ± 0.2
伞花木 *Eurycorymbus cavaleriei*	无患子科 Sapindaceae	10.6 ± 0.6	7.6 ± 0.3
青檀 *Pteroceltis tatarinowii*	榆科 Ulmaceae	15.6 ± 0.6	8.7 ± 0.2
菜豆树 *Radermachera sinica*	紫葳科 Bignoniaceae	13.5 ± 0.5	8.3 ± 0.2
圆叶乌桕 *Triadica rotundifolia*	大戟科 Euphorbiaceae	15.8 ± 4.2	8.5 ± 0.3
常绿 Evergreen			
假鱼骨木 *Psydrax dicocca*	茜草科 Rubiaceae	9.2 ± 1.1	6.5 ± 0.5
灰岩棒柄花 *Cleidion bracteosum*	大戟科 Euphorbiaceae	7.3 ± 0.3	5.2 ± 0.2
岩生厚壳桂 *Cryptocarya calcicola*	樟科 Lauraceae	8.1 ± 0.4	6.5 ± 0.2
青冈 *Cyclobalanopsis glauca*	壳斗科 Fagaceae	10.9 ± 1.2	7.4 ± 0.6
大叶水榕 *Ficus glaberrima*	桑科 Moraceae	19.5 ± 3.4	7.7 ± 0.7
山小橘 *Glycosmis pentaphylla*	芸香科 Rutaceae	6.4 ± 0.3	4.3 ± 0.3
黑木姜子 *Litsea salicifolia*	樟科 Lauraceae	7.6 ± 0.8	6.8 ± 0.4
小芸木 *Micromelum integerrimum*	芸香科 Rutaceae	6.2 ± 1.1	5.3 ± 0.8
千里香 *Murraya paniculata*	芸香科 Rutaceae	6.4 ± 0.1	5.0 ± 0.2
广西密花树 *Myrsine kwangsiensis*	紫金牛科 Myrsinaceae	7.6 ± 0.3	6.1 ± 0.2
铁榄 *Sinosideroxylon pedunculatum*	山榄科 Sapotaceae	8.8 ± 0.4	6.5 ± 0.2

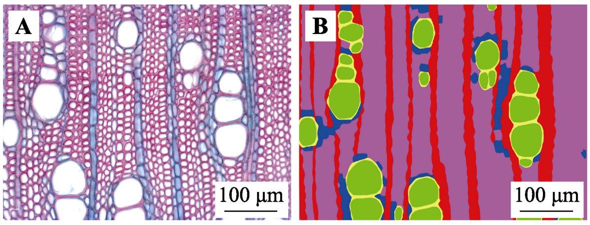

图1 菜豆树木质部染色切片(**A**)和经过人工辨别和绘制后的木质部组织结构分布图(**B**)。绿色, 导管管腔; 黄色, 导管壁; 红色, 射线细胞; 蓝色, 轴向薄壁细胞; 紫色, 纤维细胞。

Fig. 1 A stained xylem cross-section image of *Radermachera sinica* (**A**), and the same image in which different xylem tissues were manually coded with different colors (**B**). Green, vessel lumen; Yellow, vessel wall; Red, ray parenchyma; Blue, axial parenchyma; Purple, fibers.

(1)导管水力直径(*Dh*)的计算公式参照Tyree和Zimmermann (2002):

$$Dh = \sqrt[4]{\frac{\sum_{i=1}^{n} b_i^4}{n}} \tag{1}$$

式中, b_i表示单个导管长短轴直径的平均值。

(2)理论导水率(*Kt*), 反映木质部水分运输的效率性, 计算公式参照Tyree和Zimmermann (2002):

$$Kt = \frac{\rho\pi}{128\eta} \times Vd \times Dh^4 \tag{2}$$

式中, *Vd*表示导管密度; *Dh*表示导管水力直径; ρ表示20 ℃下水的密度998.2 $kg \cdot m^{-3}$; η表示20 ℃下水的黏度1.002×10^{-9} MPa·s。

1.4 数据分析

全球木本植物木质部组织比例数据从TRY Database (Kattge *et al.*, 2020)下载, 利用R 3.5.0软件进行统计分析。用ggtern软件(Hamilton & Ferry, 2018)绘制木论和全球的木质部组织比例三角坐标图; 用stats R软件中的t.test公式分析常绿与落叶树种木质部解剖结构和水力特征的差异显著性; 用factoextra软件的PCA公式做主成分分析。利用smatr R软件中的sma公式通过简化主轴回归分析(Warton *et al.*, 2012)来分析木论和全球树种木质部各组织比例之间的相关性、理论导水率与导管壁加固系数的相关性, 以及落叶与常绿树种直线回归斜率和截距的差异性。所有图用R-package软件的base绘制。

2 结果

2.1 喀斯特树种木质部解剖特征与全球木本植物数据的比较

本研究测定的喀斯特树种木质部轴向薄壁组织比例的种间变异较大(变异系数为54.6%), 最低值为2.6% (大叶紫珠(*Callicarpa macrophylla*)), 最高值为31.0% (青冈(*Cyclobalanopsis glauca*))。射线组织比例的变异系数是29.1%, 最小值是8.7% (千里香), 最大值是29.6% (灰岩棒柄花(*Cleidion bracteosum*))。导管组织比例的种间差异相对较小, 变异系数为26.2% (图2; 附录I)。铁榄(*Sinosideroxylon pedunculatum*)和青冈的导管周围有环管管胞, 其环管管胞面积分别占木质部横截面积的12.1%和12.6% (图2; 附录II)。与全球木本植物木质部组织比例数据对比分析, 本研究21种喀斯特树种木质部纤维组织和导管组织比例分别为全球数据平均值的87%和90% (图2), 但是这些喀斯特树种的木质部趋于具有较高比例的轴向薄壁组织, 其平均值是全球数据平均值的4.3倍(图2, 图3A)。

2.2 喀斯特树种木质部各组分之间的权衡关系

基于全球805种木本植物木质部解剖结构数据, 各组分比例之间存在显著的权衡关系。喀斯特树种木质部各组织比例的相关关系与全球数据的分析结果不完全一致: 喀斯特树种的纤维组织比例与薄壁组织比例存在显著的权衡关系, 但是导管组织比例与纤维组织比例和薄壁组织比例均不存在显著的相关关系(图3B)。

2.3 喀斯特常绿与落叶树种木质部水力特征的差异

主成分分析结果表明第1轴解释总变异的39%, 与木质部导管的管径(*Dh*、*Vd*)相关; 第2轴解释总变异的22%, 与木质部的贮存(*TPf*)和水分传导率(*Kt*)相关(图4A)。常绿和落叶树种在第2轴可以显著区分为两个类群, 常绿树种具有较多的轴向薄壁细胞和较低的理论导水率(p < 0.001; 图4B; 附录I)。不论常绿树种还是落叶树种, 理论导水率和导管壁加固系数之间均呈显著的负相关关系; 但是这两个植物类群的直线回归方程的截距具有显著差异(p = 0.002), 即在理论导水率相同情况下, 落叶树种具有更高的导管壁加固系数(图5)。

DOI: 10.17521/cjpe.2020.0367

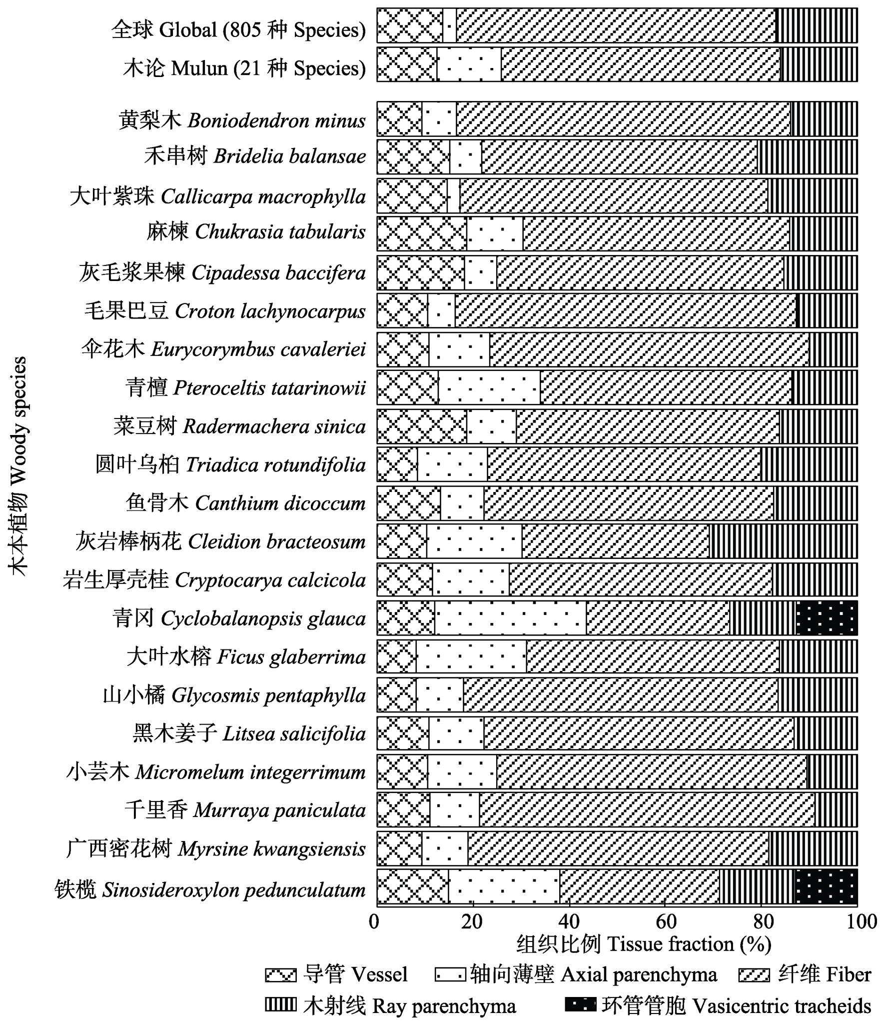

图2 基于TRY Database数据库的全球805种木本植物木质部各组分比例的平均值和广西木论21种喀斯特树种的木质部各组分的比例。

Fig. 2 Xylem tissue partitioning of the 21 karst woody species in Mulun, Guangxi, and 805 woody species data downloaded from the TRY Database.

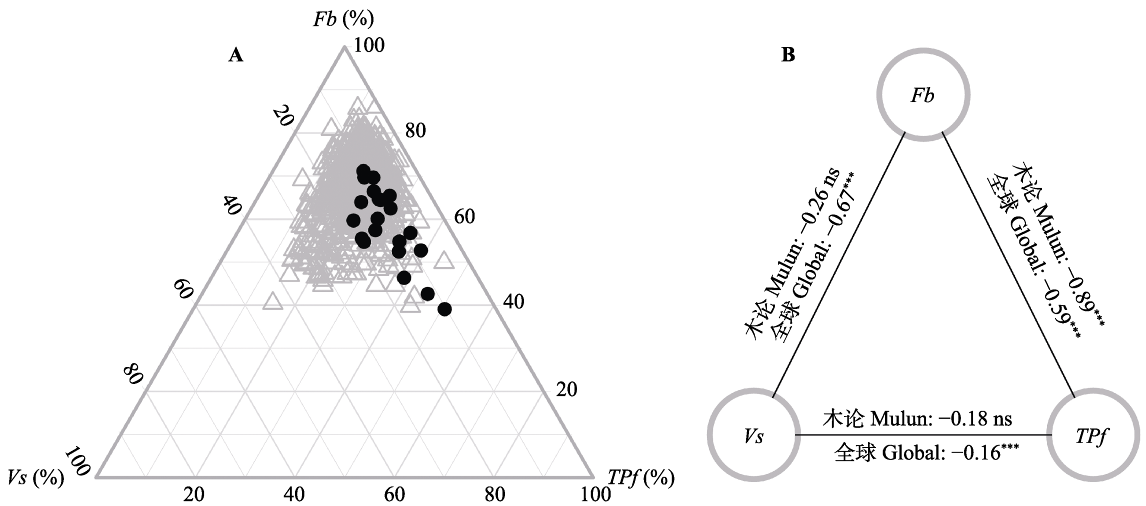

图3 喀斯特树种在全球木质部组织划分谱的位置(**A**)和木质部各组织比例之间的相关性(**B**)。●, 喀斯特树种; △, 全球数据(TRY)。*Fb,* 纤维组织比例; *TPf,* 薄壁组织比例; *Vs,* 导管组织比例。ns, $p > 0.05$; ***, $p < 0.001$。

Fig. 3 Distributions of the karst woody species in the global xylem partitioning spectrum (**A**) and relationships among xylem tissue fractions (**B**). ●, karst woody species; △, global observations from TRY. *Fb,* fibers fraction; *TPf,* total parenchyma fraction; *Vs,* vessels fraction. ns, $p > 0.05$; ***, $p < 0.001$.

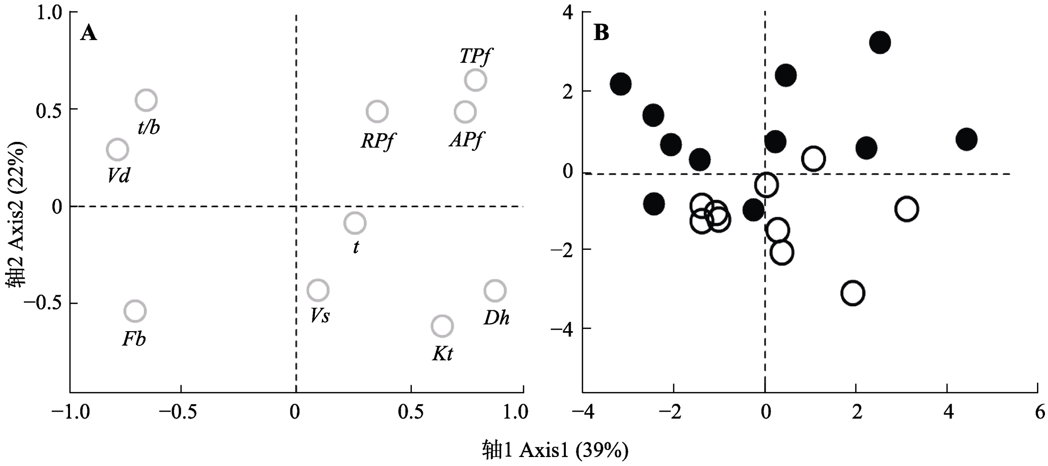

图4 广西木论喀斯特木本植物10个木质部性状(**A**)和21个树种(**B**)的主成分分析图。○, 落叶树种; ●, 常绿树种。*APf*, 轴向薄壁组织比例; *Dh*, 导管水力直径; *Fb*, 纤维组织比例; *Kt*, 理论导水率; *RPf*, 射线组织比例; *t*, 相连接两个导管的细胞壁厚度之和; *t/b*, 导管壁加固系数; *TPf*, 总的薄壁组织比例; *Vd*, 导管密度; *Vs*, 导管组织比例。

Fig. 4 Principal component analysis for 10 xylem traits of woody plant (**A**), and 21 karst woody species (**B**) in Mulun, Guangxi. ○, deciduous; ●, evergreen. *APf*, axial parenchyma fraction; *Dh*, hydraulically-mean vessel diameter; *Fb*, fiber fraction; *Kt*, theoretical hydraulic conductivity; *RPf*, ray parenchyma fraction; *t*, double wall thickness measured from vessel pairs; *t/b*, vessel wall reinforcement coefficient; *TPf*, total parenchyma fraction; *Vd*, vessel density; *Vs*, vessel lumen fraction.

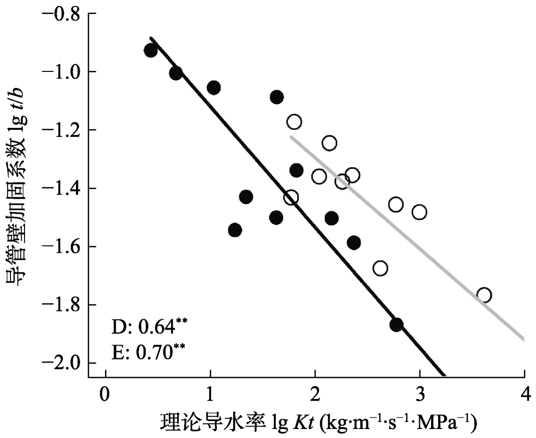

图5 广西木论喀斯特21个树种导管壁加固系数(*t/b*)与理论导水率(*Kt*)的相关关系的简化主轴回归分析。○: 落叶树种(D), ●: 常绿树种(E)。落叶树种回归方程(灰色): $y = -0.31x - 0.67$, 常绿树种回归方程(黑色): $y = -0.41x - 0.71$。**, $p < 0.01$。

Fig. 5 Reduced major axis regression of vessel wall reinforcement coefficient (*t/b*) and theoretical hydraulic conductivity (*Kt*) of 21 karst woody species in Mulun, Guangxi. ○, deciduous (D); ●, evergreen (E). Linear regression of deciduous species (grey): $y = -0.31x - 0.67$; linear regression of evergreen species (black): $y = -0.41x - 0.71$. **, $p < 0.01$.

3 讨论

3.1 喀斯特树种木质部具有较小的导管水力直径和较大比例的轴向薄壁组织

与全球木本植物木质部解剖结构数据相比, 喀斯特树木的木质部趋于具有较高比例的轴向薄壁组织(图2)。已有研究表明薄壁组织具有贮存水分、储存和转运碳水化合物的功能(Plavcová & Jansen, 2015; Morris *et al*., 2016b), 在维持植物水分平衡(Meinzer *et al*., 2009)和修复导管栓塞过程中发挥重要作用(Zwieniecki & Holbrook, 2009; Tomasella *et al*., 2019)。木质部中高的薄壁组织比例具有高的水容(Secchi *et al*., 2017; Santiago *et al*., 2018), 当土壤有效水分供给不足时, 高的水容可以缓解土壤与叶片的水势差, 从而维持叶片的气体交换(McCulloh *et al*., 2019; Siddiq *et al*., 2019)。最近对温带石灰岩山地的19种阔叶树种的研究发现, 木质部薄壁细胞比例与抗栓塞能力具有显著的负相关关系(Chen *et al*., 2020)。以上研究结果证明了薄壁细胞的贮存能力对喀斯特树种的干旱适应具有重要作用(谭凤森等, 2019), 也解释了中亚热带喀斯特树种较低的抗栓塞能力(Fan *et al*., 2011)。

本研究中喀斯特21种树种木质部导管水力直径(平均值为44.76 μm)显著地低于全球木本植物的平均值(94.43 μm; Morris *et al*., 2018)。在西南热带喀斯特森林的研究也发现喀斯特树种的导管直径要显著地低于临近的沟谷雨林树种(Zhu *et al*., 2017), 体现了对喀斯特旱生生境的水力适应(Hacke *et al*., 2017)。与其他树种不同, 青冈和铁榄的木质部导管周围具有直径较小的环管管胞(图2), 而且它们主要分布在喀斯特峰丛洼地上坡更为干旱的生境。同样,

DOI: 10.17521/cjpe.2020.0367

在加利福尼亚南部干旱灌木林(Hacke, 2015)和海南红树林(邓传远等, 2015)也发现优势树种木质部存在环管管胞。环管管胞本身除了具有水分运输的功能外, 当植物面临水分胁迫时还能够连接被栓塞阻隔的导管, 从而保证了水分运输的安全性(Carlquist, 2001)。喀斯特树种的环管管胞的生理作用值得进一步探讨。

3.2 喀斯特树种木质部各组分间的权衡关系

与全球数据的分析结果不同, 喀斯特树种木质部导管组织比例与其他组织比例之间的相关性均不显著(图3)。这一结果与加利福尼亚干旱森林树种的研究结果(Pratt & Jacobsen, 2017)相似, 可能与这些木本植物具有相对稳定的导管组织比例有关。喀斯特树种木质部纤维组织比例与薄壁组织比例存在显著的权衡关系(图3), 这些树种的木质部倾向于具有较高的薄壁组织比例而不是纤维组织, 它们可能通过提高栓塞修复能力(而非抗栓塞能力)适应干旱(Pratt & Jacobsen, 2017; Janssen *et al*., 2020; Aritsara *et al*., 2021)。较低的纤维组织比例(支撑作用)也从木质部结构的角度解释了为什么中亚热带的喀斯特森林冠层高度要显著低于同区域的亚热带常绿阔叶林(平均林冠高度为28.90 m; Liu *et al*., 2019)。

3.3 喀斯特落叶与常绿树种木质部解剖和水力特征的差异

本研究发现喀斯特落叶与常绿树种的导管水力直径和导管密度没有显著差异, 但是落叶树种的理论导水率是常绿树种的两倍(附录I)。根据Hagen-Poiseuille定理, 理论导水率与导管直径的4次方成正比, 导管直径的较小差异(喀斯特落叶树种比常绿树种的平均值高25%), 导致理论导水率的较大变化。本研究发现木质部水分运输效率性(理论导水率)与安全性(导管壁加固系数)之间存在权衡关系, 但是落叶与常绿树种具有显著差异: 若导管壁加固系数相同, 落叶树种具有较高的水分运输效率; 如导水率相同, 常绿树种反而具有较低的抗栓塞能力。这与以往研究发现同一森林中常绿植物比落叶植物具有更强的抗栓塞能力的结果相反(Chen *et al*., 2009; Fu *et al*., 2012), 原因可能在于本研究的喀斯特常绿树种具有丰富的轴向薄壁细胞(附录I), 并不依赖强的抗栓塞能力适应干旱。

通过长期的隔离降雨模拟试验, 结果发现干旱加剧会导致热带季节性森林中落叶植物成分显著增加(Aguirre-Gutiérrez *et al*., 2019)。在气候变化背景下, 我国亚热带地区呈现显著的干热化趋势(Qu & Huang, 2018; Yin *et al*., 2018)。由于亚热带喀斯特森林对气候变化的响应较为敏感, 干旱程度的增加将会影响喀斯特森林群落的组成和物种多样性, 并进一步影响森林生态系统的结构和功能。基于喀斯特树种木质部解剖结构和水力特征的研究有助于了解它们对干旱的水力适应, 从而提高对树种动态变化的预测性。

4 结论

本研究揭示了中亚热带喀斯特森林树种木质部普遍具有较高比例的薄壁组织, 表明薄壁组织的贮存和修复能力对维持喀斯特树种木质部的水力安全至关重要。对喀斯特常绿和落叶树种木质部特征的比较结果表明, 落叶树种木质部倾向于提高水分运输效率, 而常绿树种则倾向于投资更多的薄壁组织用于调节水分平衡。结合喀斯特树种木质部功能性状与树种动态变化(生长和死亡)的研究有助于理解喀斯特森林对气候变化的响应。

致谢 感谢广西大学林学院的宋慧清、曾文豪和张启伟同学在野外采样和实验测定工作中给予的帮助。

参考文献

Aguirre-Gutiérrez J, Oliveras I, Rifai S, Fauset S, Adu-Bredu S, Affum-Baffoe K, Baker TR, Feldpausch TR, Gvozdevaite A, Hubau W, Kraft NJB, Lewis SL, Moore S, Niinemets Ü, Peprah T, Phillips OL, Ziemińska K, Enquist B, Malhi Y (2019). Drier tropical forests are susceptible to functional changes in response to a long-term drought. *Ecology Letters,* 22, 855-865.

Aritsara ANA, Razakandraibe VM, Ramananantoandro T, Gleason SM, Cao KF (2021). Increasing axial parenchyma fraction in the Malagasy Magnoliids facilitated the co-optimization of hydraulic efficiency and safety. *New Phytologist,* 229, 1467-1480.

Barbosa ACF, Pace MR, Witovisk L, Angyalossy V (2010). A new method to obtain good anatomical slides of heterogeneous plant parts. *IAWA Journal,* 31, 373-383.

Cao KF, Fu PL, Chen YJ, Jiang YJ, Zhu SD (2014). Implications of the ecophysiological adaptation of plants on tropical karst habitats for the ecological restoration of desertified rocky lands in Southern China. *Scientia Sinica Vitae,* 44, 238-247. [曹坤芳, 付培立, 陈亚军, 姜艳娟, 朱师丹 (2014). 热带岩溶植物生理生态适应性对于南方石漠化

土地生态重建的启示. 中国科学: 生命科学, 44, 238-247.]

Cao M, Wu C, Liu JC, Jiang YJ (2020). Increasing leaf δ^{13}C values of woody plants in response to water stress induced by tunnel excavation in a karst trough valley: implication for improving water-use efficiency. *Journal of Hydrology,* 586, 124895. DOI: 10.1016/j.jhydrol.2020.124895.

Carlquist S (2018). Living cells in wood 3. Overview; Functional anatomy of the parenchyma network. *Botanical Review,* 84, 242-294.

Carlquist SJ (2001). *Comparative Wood Anatomy*. Springer, Berlin. 448.

Chen HS, Nie YP, Wang KL (2013). Spatio-temporal heterogeneity of water and plant adaptation mechanisms in karst regions: a review. *Acta Ecologica Sinica,* 33, 317-326. [陈洪松, 聂云鹏, 王克林 (2013). 岩溶山区水分时空异质性及植物适应机理研究进展. 生态学报, 33, 317-326.]

Chen ZC, Li S, Luan JW, Zhang YT, Zhu SD, Wan XC, Liu SR (2019). Prediction of temperate broadleaf tree species mortality in arid limestone habitats with stomatal safety margins. *Tree Physiology,* 39, 1428-1437.

Chen ZC, Zhu SD, Zhang YT, Luan JW, Li S, Sun PS, Wan XC, Liu SR (2020). Tradeoff between storage capacity and embolism resistance in the xylem of temperate broadleaf tree species. *Tree Physiology,* 40, 1029-1042.

Choat B, Ball MC, Luly JG, Holtum JAM (2005). Hydraulic architecture of deciduous and evergreen dry rainforest tree species from north-eastern Australia. *Trees,* 19, 305-311.

Deng CY, Zheng JM, Zhang WC, Guo SZ, Xue QH, Ye LY, Sun JW (2015). Ecological wood anatomy of *Rhizophora stylosa*. *Chinese Journal of Plant Ecology,* 39, 604-615. [邓传远, 郑俊鸣, 张万超, 郭素枝, 薛秋华, 叶露莹, 孙建文 (2015). 红海榄木材结构的生态解剖. 植物生态学报, 39, 604-615.]

Fan DY, Jie SL, Liu CC, Zhang XY, Xu XW, Zhang SR, Xie ZQ (2011). The trade-off between safety and efficiency in hydraulic architecture in 31 woody species in a karst area. *Tree Physiology,* 31, 865-877.

Fu PL, Jiang YJ, Wang AY, Brodribb TJ, Zhang JL, Zhu SD, Cao KF (2012). Stem hydraulic traits and leaf water-stress tolerance are co-ordinated with the leaf phenology of angiosperm trees in an Asian tropical dry karst forest. *Annals of Botany,* 110, 189-199.

Geekiyanage N, Goodale UM, Cao KF, Kitajima K (2019). Plant ecology of tropical and subtropical karst ecosystems. *Biotropica,* 51, 626-640.

Godfrey JM, Riggio J, Orozco J, Guzmán-Delgado P, Chin ARO, Zwieniecki MA (2020). Ray fractions and carbohydrate dynamics of tree species along a 2750 m elevation gradient indicate climate response, not spatial storage limitation. *New Phytologist,* 225, 2314-2330.

Hacke UG (2015). *Functional and Ecological Xylem Anatomy*. Springer International Publishing, Cham, Switzerland.

Hacke UG, Sperry JS (2001). Functional and ecological xylem anatomy. *Perspectives in Plant Ecology, Evolution and Systematics,* 4, 97-115.

Hacke UG, Sperry JS, Pockman WT, Davis SD, McCulloh KA (2001). Trends in wood density and structure are linked to prevention of xylem implosion by negative pressure. *Oecologia,* 126, 457-461.

Hacke UG, Spicer R, Schreiber SG, Plavcová L (2017). An ecophysiological and developmental perspective on variation in vessel diameter. *Plant, Cell & Environment,* 40, 831-845.

Hamilton NE, Ferry M (2018). Ggtern: Ternary Diagrams Using ggplot2. *Journal of Statistical Software,* 87, 1-17.

Hu BQ (2014). *Study on Human-Land Systems in Karst Areas*. Science Press, Beijing. 596. [胡宝清 (2014). 喀斯特人地系统研究. 科学出版社, 北京. 596.]

Janssen TAJ, Hölttä T, Fleischer K, Naudts K, Dolman H (2020). Wood allocation trade-offs between fiber wall, fiber lumen, and axial parenchyma drive drought resistance in neotropical trees. *Plant, Cell & Environment,* 43, 965-980.

Jiang ZC, Li XK, Zeng FP (2007). *Ecological Reconstruction in Peak Cluster Karst Depression.* Geological Publishing House, Beijing. 151. [蒋忠诚, 李先琨, 曾馥平 (2007). 岩溶峰丛洼地生态重建. 地质出版社, 北京. 151.]

Kattge J, Bönisch G, Diaz S, Lavorel S, Prentice I, Leadley P (2020). TRY plant trait database—Enhanced coverage and open access. *Global Change Biology,* 26, 119-188.

Liu H, Gleason SM, Hao GY, Hua L, He PC, Goldstein G, Ye Q (2019). Hydraulic traits are coordinated with maximum plant height at the global scale. *Science Advances,* 5, eaav1332. DOI: 10.1126/sciadv.aav1332.

Liu L, Song TQ, Peng WX, Wang KL, Du H, Lu SY, Zeng FP (2012). Spatial heterogeneity of soil microbial biomass in Mulun National Nature Reserve in karst area. *Acta Ecologica Sinica,* 32, 207-214. [刘璐, 宋同清, 彭晚霞, 王克林, 杜虎, 鹿士杨, 曾馥平 (2012). 木论喀斯特自然保护区土壤微生物生物量的空间格局. 生态学报, 32, 207-214.]

Liu SJ, Zhang W, Wang KL, Chen HS, Wei GF (2010). Spatiotemporal heterogeneity and its formation causes of soil physical properties in karst peak-cluster depression area of northwest Guangxi, China. *Chinese Journal of Applied Ecology,* 21, 2249-2256. [刘淑娟, 张伟, 王克林, 陈洪松, 韦国富 (2010). 桂西北喀斯特峰丛洼地土壤物理性质的时空分异及成因. 应用生态学报, 21, 2249-2256.]

McCulloh KA, Domec JC, Johnson DM, Smith DD, Meinzer FC (2019). A dynamic yet vulnerable pipeline: integration and coordination of hydraulic traits across whole plants. *Plant, Cell & Environment,* 42, 2789-2807.

Meinzer FC, Johnson DM, Lachenbruch B, McCulloh KA, Woodruff DR (2009). Xylem hydraulic safety margins in

DOI: 10.17521/cjpe.2020.0367

woody plants: coordination of stomatal control of xylem tension with hydraulic capacitance. *Functional Ecology,* 23, 922-930.

Morris H, Gillingham MAF, Plavcová L, Gleason SM, Olson ME, Coomes DA, Fichtler E, Klepsch MM, Martínez-Cabrera HI, McGlinn DJ, Wheeler EA, Zheng JM, Ziemińska K, Jansen S (2018). Vessel diameter is related to amount and spatial arrangement of axial parenchyma in woody angiosperms. *Plant, Cell & Environment,* 41, 245-260.

Morris H, Brodersen C, Schwarze FWMR, Jansen S (2016a). The parenchyma of secondary xylem and its critical role in tree defense against fungal decay in relation to the CODIT model. *Frontiers in Plant Science,* 7, 1665. DOI: 10.3389/fpls.2016.01665.

Morris H, Plavcová L, Cvecko P, Fichtler E, Gillingham MAF, Martínez-Cabrera HI, McGlinn DJ, Wheeler E, Zheng JM, Ziemińska K, Jansen S (2016b). A global analysis of parenchyma tissue fractions in secondary xylem of seed plants. *New Phytologist,* 209, 1553-1565.

Peng WX, Wang KL, Song TQ, Zeng FP, Wang JR (2008). Controlling and restoration models of complex degradation of vulnerable karst ecosystem. *Acta Ecologica Sinica,* 28, 811-820. [彭晚霞, 王克林, 宋同清, 曾馥平, 王久荣 (2008). 喀斯特脆弱生态系统复合退化控制与重建模式. 生态学报, 28, 811-820.]

Pérez-Harguindeguy N, Díaz S, Garnier E, Lavorel S, Poorter H, Jaureguiberry P, Bret-Harte MS, Cornwell WK, Craine JM, Gurvich DE, Urcelay C, Veneklaas EJ, Reich PB, Poorter L, Wright IJ, *et al*. (2013). New handbook for standardised measurement of plant functional traits worldwide. *Australian Journal of Botany,* 61, 167. DOI: 10.1071/bt12225.

Plavcová L, Hoch G, Morris H, Ghiasi S, Jansen S (2016). The amount of parenchyma and living fibers affects storage of nonstructural carbohydrates in young stems and roots of temperate trees. *American Journal of Botany,* 103, 603-612.

Plavcová L, Jansen S (2015). The role of xylem parenchyma in the storage and utilization of nonstructural carbohydrates// Hacke U. *Functional and Ecological Xylem Anatomy*. Springer International Publishing, Cham, Switzerland. 209-234.

Pratt RB, Jacobsen AL (2017). Conflicting demands on angiosperm xylem: tradeoffs among storage, transport and biomechanics. *Plant, Cell & Environment,* 40, 897-913.

Qu X, Huang G (2018). Different multi-year mean temperature in mid-summer of South China under different 1.5 °C warming scenarios. *Scientific Reports,* 8, 13794. DOI: 10.1038/s41598-018-32277-6.

Rueden CT, Hiner MC, Eliceiri KW (2016). ImageJ: image analysis interoperability for the next generation of biological image data. *Microscopy and Microanalysis,* 22, 2066-2067.

Santiago LS, de Guzman ME, Baraloto C, Vogenberg JE, Brodie M, Hérault B, Fortunel C, Bonal D (2018). Coordination and trade-offs among hydraulic safety, efficiency and drought avoidance traits in Amazonian rainforest canopy tree species. *New Phytologist,* 218, 1015-1024.

Secchi F, Pagliarani C, Zwieniecki MA (2017). The functional role of xylem parenchyma cells and aquaporins during recovery from severe water stress. *Plant, Cell & Environment,* 40, 858-871.

Siddiq Z, Zhang YJ, Zhu SD, Cao KF (2019). Canopy water status and photosynthesis of tropical trees are associated with trunk sapwood hydraulic properties. *Plant Physiology and Biochemistry,* 139, 724-730.

Song TQ (2015). *Plants and Environment in Karst Areas of Southwest China*. Science Press, Beijing. 607. [宋同清 (2015). 西南喀斯特植物与环境. 科学出版社, 北京. 607.]

Tan FS, Song HQ, Li ZG, Zhang QW, Zhu SD (2019). Hydraulic safety margin of 17 co-occurring woody plants in a seasonal rain forest in Guangxi's Southwest karst landscape, China. *Chinese Journal of Plant Ecology,* 43, 227-237. [谭凤森, 宋慧清, 李忠国, 张启伟, 朱师丹 (2019). 桂西南喀斯特季雨林木本植物的水力安全. 植物生态学报, 43, 227-237.]

Tomasella M, Petrussa E, Petruzzellis F, Nardini A, Casolo V (2019). The possible role of non-structural carbohydrates in the regulation of tree hydraulics. *International Journal of Molecular Sciences,* 21, E144. DOI: 10.3390/ijms21010144.

Tyree MT, Zimmermann MH (2002). *Xylem Structure and the Ascent of Sap*. 2nd ed. Springer Heidelberg, Berlin.

Wang J, Wen XF, Zhang XY, Li SG (2018). The strategies of water-carbon regulation of plants in a subtropical primary forest on karst soils in China. *Biogeosciences,* 15, 4193-4203.

Warton DI, Duursma RA, Falster DS, Taskinen S (2012). Smatr 3—An R package for estimation and inference about allometric lines. *Methods in Ecology and Evolution,* 3, 257-259.

Yin YH, Ma DY, Wu SH (2018). Climate change risk to forests in China associated with warming. *Scientific Reports,* 8, 493. DOI: 10.1038/s41598-017-18798-6.

Yuan DX (1992). Karst in southwest China and its comparison with karst in North China. *Quaternary Sciences,* 12, 352-361. [袁道先 (1992). 中国西南部的岩溶及其与华北岩溶的对比. 第四纪研究, 12, 352-361.]

Zheng YW (1999). *Introduction to Mulun Karst Forest Region.* Science Press, Beijing. 254. [郑颖吾 (1999). 木论喀斯特林区概论. 科学出版社, 北京. 254.]

Zhou CB, Hu X, Song YY, Gong W, Hu TX (2016). Radial variation and its storage function of ray tissue. *Journal of Northwest Forestry University,* 31, 179-183. [周朝彬, 胡霞, 宋于洋, 龚伟, 胡庭兴 (2016). 射线组织径向变异及其贮藏功能研究进展. 西北林学院学报, 31, 179-183.]

Zhu SD, Chen YJ, Fu PL, Cao KF (2017). Different hydraulic traits of woody plants from tropical forests with contrasting soil water availability. *Tree Physiology,* 37, 1469-1477.

Zwieniecki MA, Holbrook NM (2009). Confronting Maxwell's demon: biophysics of xylem embolism repair. *Trends in Plant Science,* 14, 530-534.

特邀编委: 黄建国　责任编辑: 李　敏

附录 I　21 个喀斯特树种的木质部特征(平均值±标准差)

Supplement I　Xylem characteristics of the 21 karst woody species from Mulun, Guangxi (mean ± *SD*)

https://www.plant-ecology.com/fileup/1005-264X/PDF/cjpe.2020.0367-S1.pdf

附录 II　广西木论 21 种喀斯特树种的木质部染色切片图

Supplement II　Xylem anatomical structure the 21 karst woody species in Mulun, Guangxi

https://www.plant-ecology.com/fileup/1005-264X/PDF/cjpe.2020.0367-S2.pdf

DOI: 10.17521/cjpe.2020.0367

10.17521/cjpe.2020.0367-S1

倪鸣源, Aritsara ANA, 王永强, 黄冬柳, 项伟, 万春燕, 朱师丹 (2021). 中亚热带喀斯特常绿落叶阔叶混交林典型树种的木质部解剖与功能特征分析. 植物生态学报, 45, 394-403. DOI: 10.17521/cjpe.2020.0367

Ni MY, Aritsara ANA, Wang YQ, Huang DL, Xiang W, Wan CY, Zhu SD (2021). An analysis of xylem anatomy and function of representative tree species in a mixed evergreen and deciduous broad-leaved forest of mid-subtropical karst region. *Chinese Journal of Plant Ecology*, 45, 394-403. DOI: 10.17521/cjpe.2020.0367

https://www.plant-ecology.com/CN/10.17521/cjpe.2020.0367

附录I　广西木论21个喀斯特树种的木质部特征(平均值±标准差)

Supplement I　Xylem characteristics of the 21 karst woody species from Mulun, Guangxi (mean ± *SD*)

物种 Species	*Vs*	*APf*	*Fb*	*RPf*	*TPf*	*Tr*	*Dh*	*Vd*	*Kt*	*t*	*t*/*b*
黄梨木 *Boniodendron minus*	9.1 ± 0.5	6.9 ± 0.8	67.3 ± 1.8	13.4 ± 1.3	20.3 ± 1.5	—	42.7 ± 2.3	71.1 ± 5.6	5.9 ± 0.9	9.5 ± 0.6	0.24 ± 0.01
禾串树 *Bridelia balansae*	14.4 ± 1.4	6.4 ± 2.1	54.8 ± 3.0	19.8 ± 0.6	26.2 ± 1.9	—	46.2 ± 1.8	74.1 ± 8.0	8.4 ± 1.2	11.6 ± 1.5	0.29 ± 0.02
大叶紫珠 *Callicarpa macrophylla*	13.9 ± 1.5	2.6 ± 0.3	60.7 ± 1.7	17.7 ± 0.9	20.3 ± 0.8	—	39.7 ± 2.2	126.7 ± 14.9	7.6 ± 1.2	9.1 ± 0.5	0.26 ± 0.03
麻楝 *Chukrasia tabularis*	17.7 ± 2.6	10.9 ± 3.6	52.2 ± 5.6	13.3 ± 1.4	24.2 ± 3.4	—	48.1 ± 5.9	113.6 ± 18.5	15.9 ± 4.6	9.9 ± 0.4	0.23 ± 0.02
灰毛浆果楝 *Cipadessa baccifera*	17 ± 1.7	6.1 ± 0.6	55.4 ± 2.5	14.3 ± 0.5	20.4 ± 0.7	—	42.5 ± 2.7	142.4 ± 22.0	10.5 ± 1.2	9.3 ± 0.5	0.26 ± 0.02
毛果巴豆 *Croton lachynocarpus*	10.2 ± 0.7	5.4 ± 1.7	67.9 ± 0.6	12.0 ± 1.1	17.4 ± 1.0	—	45.5 ± 3.0	58.5 ± 9.0	6.0 ± 1.0	11.4 ± 1.1	0.31 ± 0.02
伞花木 *Eurycorymbus cavaleriei*	10.5 ± 1.0	12 ± 3.0	63.9 ± 2.8	9.8 ± 0.7	21.8 ± 2.8	—	54.8 ± 3.1	53.7 ± 6.3	13.7 ± 4.2	9.7 ± 0.6	0.19 ± 0.01
青檀 *Pteroceltis tatarinowii*	12.3 ± 1.6	20.2 ± 5.5	50.3 ± 6.9	13.0 ± 1.4	33.3± 6.5	—	46.8 ± 3.4	74.0 ± 4.1	9.6 ± 2.4	9.8 ± 1.1	0.25 ± 0.03
菜豆树 *Radermachera sinica*	17.9 ± 1.5	9.9 ± 1.5	52.3 ± 3.3	15.5 ± 1.0	25.4 ± 1.2	—	61.5 ± 6.1	105.7 ± 20.0	37.0 ± 9.1	8.7 ± 0.7	0.17 ± 0.02
圆叶乌桕 *Triadica rotundifolia*	8.2 ± 0.7	14.3 ± 1.2	55.4 ± 3.7	19.6 ± 1.7	34.0 ± 2.7	—	81.6 ± 5.4	18.6 ± 3.0	19.9 ± 3.7	13.3 ± 0.4	0.23 ± 0.03
假鱼骨木 *Psydrax dicocca*	12.6 ± 0.9	8.6 ± 2.3	57.1 ± 2.5	16.7 ± 0.7	25.3 ± 2.6	—	31.7 ± 1.5	153.0 ± 15.9	3.8 ± 0.6	7.1 ± 0.4	0.24 ± 0.02
灰岩棒柄花 *Cleidion bracteosum*	9.9 ± 1.3	19.0 ± 0.8	37.5 ± 1.7	29.6 ± 1.4	48.6 ± 1.5	—	43.4 ± 2.7	69.6 ± 5.5	6.2 ± 1.0	10.1 ± 1.1	0.26 ± 0.01
岩生厚壳桂 *Cryptocarya calcicola*	11.2 ± 2.1	15.3 ± 3.5	52.7 ± 6.3	17.0 ± 1.1	32.3 ± 3.7	—	38.7 ± 1.2	96.3 ± 15.4	5.1 ± 0.4	7.9 ± 0.3	0.22 ± 0.01
青冈 *Cyclobalanopsis glauca*	11.7 ± 1.4	31.0 ± 2.3	29.2 ± 0.9	13.5 ± 0.6	44.5 ± 2.0	12.6 ± 1.1	68.4 ± 3.3	29.3 ± 2.6	16.0 ± 2.8	6.9 ± 0.6	0.15 ± 0.03
大叶水榕 *Ficus glaberrima*	8.1 ± 0.5	22.3 ± 2.6	51.6 ± 3.0	15.9 ± 1.1	38.2 ± 2.8	—	57.6 ± 3.5	40.8 ± 4.3	10.7 ± 1.4	9.1 ± 0.7	0.20 ± 0.01
山小橘 *Glycosmis pentaphylla*	7.8 ± 1.0	9.4 ± 1.5	62.2 ± 3.1	15.7 ± 0.5	25.1 ± 1.9	—	26.9 ± 0.4	156.4 ± 27.9	2.0 ± 0.3	8.9 ± 0.5	0.37 ± 0.03
黑木姜子 *Litsea salicifolia*	10.5 ± 0.9	11.0 4.1	62.5 ± 4.3	12.8 ± 1.1	23.8 ± 4.8	—	47.0 ± 4.0	80.5 ± 15.2	8.6 ± 1.5	9.7 ± 0.4	0.22 ± 0.01

小芸木 *Micromelum integerrimum*	9.9 ± 1.1	13.6 ± 2.2	60.6 ± 4.6	10.0 ± 0.9	23.5 ± 2.8	—	30.0 ± 0.7	141.4 ± 9.8	2.8 ± 0.2	9.5 ± 0.3	0.35 ± 0.01
千里香 *Micromelum paniculata*	10.8 ± 1.0	9.8 ± 1.3	67.1 ± 2.9	8.7 ± 0.8	18.4 ± 1.7	—	30.4 ± 1.9	158.8 ± 21.2	3.4 ± 0.9	5.8 ± 0.3	0.21 ± 0.01
广西密花树 *Myrsine kwangsiensis*	8.8 ± 0.9	8.9 ± 1.5	58.0 ± 1.8	17.2 ± 2.6	26.1 ± 1.4	—	22.9 ± 1.6	235.0 ± 37.9	1.5 ± 0.2	7.9 ± 0.6	0.40 ± 0.04
铁榄 *Sinosideroxylon pedunculatum*	13.8 ± 0.8	21.5 ± 1.8	31.1 ± 1.6	14.6 ± 0.8	36.1 ± 1.1	12.1 ± 0.5	33.8 ± 1.4	157.0 ± 6.7	5.1 ± 0.7	11.2 ± 0.8	0.34 ± 0.03
变异系数 *CV*	26.2	54.6	19.7	29.1	30.5	315.9	31.9	52.3	84.2	33.7	24.8
落叶Deciduous	13.1 ± 1.2	9.5 ± 1.6	58.0 ± 2.1	14.9 ± 1.1	24.3 ± 1.8	—	51.0 ± 4.0	83.8 ± 11.9	13.5 ± 3.0	10.2 ± 0.5	0.24 ± 0.01
常绿Evergreen	10.5 ± 0.6	15.5 ± 2.2	52.0 ± 4.0	15.6 ± 1.6	31.1 ± 2.9	—	39.2 ± 4.0	119.8 ± 18.6	6.0 ± 1.3	8.6 ± 0.5	0.27 ± 0.02
显著性水平Significance level	ns	*	ns	ns	ns	—	ns	ns	*	*	ns

*, $p < 0.05$; ns, 无显著差异。*APf*, 轴向薄壁组织比例; *CV*,变异系数; *Dh*, 导管水力直径; *Fb*, 纤维组织比例; *Kt*, 理论导水率; *Rpf*, 射线组织比例; *t*, 相连接两个导管的细胞壁厚度之和; *t/b*, 导壁加固系数, *Tpf*, 总的薄壁细胞比例; *Tr*, 环管管胞比例; *Vd*, 导管密度; *Vs*, 导管组织比例;。

One asterisk (*) indicates significant difference ($p < 0.05$) and *ns*, indicates non-significant difference ($p > 0.05$). *APf*, axial parenchyma fraction; *CV*, Coefficient of Variation *Dh*, hydraulically-mean vessel diameter; *Fb*, fiber fraction; *Kt*, theoretical hydraulic conductivity; *RPf*, ray parenchyma fraction; *t*, double wall thickness measured from vessel pairs; *t/b*, vessel wall reinforcement coefficient; *TPf*, total parenchyma fraction; *Tr*, vasicentric tracheid fraction; *Vd*, vessel density; *Vs*, vessel lumen fraction;

倪鸣源, Aritsara ANA**,** 王永强, 黄冬柳, 项伟, 万春燕, 朱师丹 **(2021).** 中亚热带喀斯特常绿落叶阔叶混交林典型树种的木质部解剖与功能特征分析. 植物生态学报**, 45, 394-403. DOI: 10.17521/cjpe.2020.0367**

Ni MY, Aritsara ANA, Wang YQ, Huang DL, Xiang W, Wan CY, Zhu SD (2021). An analysis of xylem anatomy and function of representative tree species in a mixed evergreen and deciduous broad-leaved forest of mid-subtropical karst region. *Chinese Journal of Plant Ecology*, 45, 394-403. DOI: 10.17521/cjpe.2020.0367

https://www.plant-ecology.com/CN/10.17521/cjpe.2020.0367

附录 **II** 广西木论 **21** 种喀斯特树种的木质部染色切片图

Supplement II Xylem anatomical structure the 21 karst woody species in Mulun, Guangxi

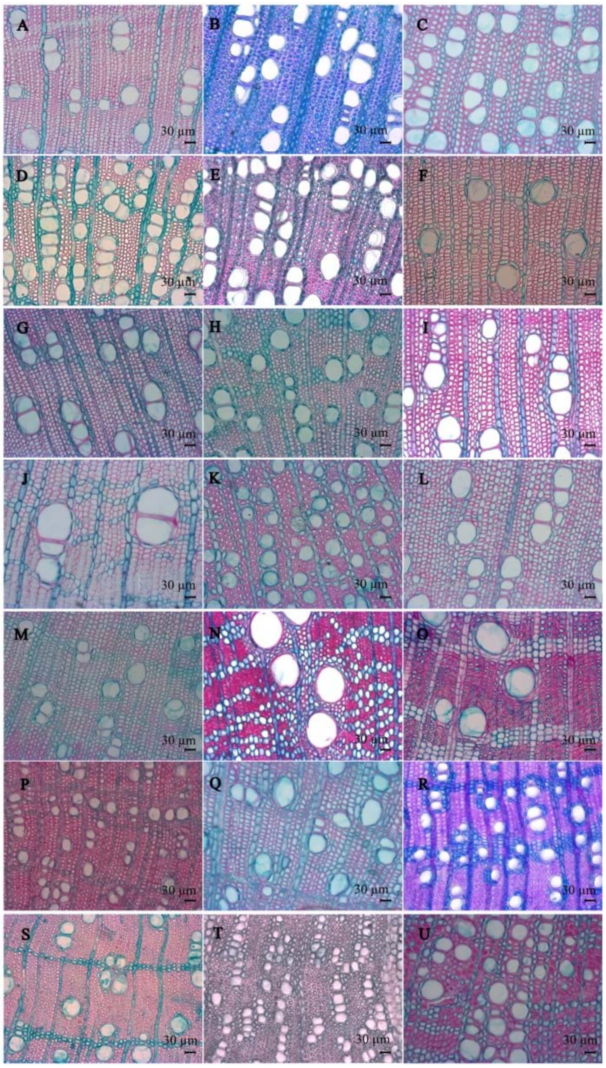

A, 黄梨木。**B,** 禾串树。**C,** 大叶紫珠。**D,** 麻楝。 **E,** 灰毛浆果楝。**F,** 毛果巴豆。**G,** 伞花木。**H,** 青檀。**I,** 菜豆树。**J,** 圆叶乌桕。**K,** 假鱼骨木。**L,** 灰岩棒柄花。**M,** 岩生厚壳桂。**N,** 青冈。**O,** 大叶水榕。**P,** 山小橘。**Q,** 黑木姜子。**R,** 小芸木。**S,** 千里香。**T,** 广西密花树。**U,** 铁榄。

A, *Boniodendron minus*. **B,** *Bridelia balansae*. **C,** *Callicarpa macrophylla*. **D,** *Chukrasia tabularis*. **E,** *Cipadessa baccifera*. **F,***Croton lachynocarpus*. **G,** *Eurycorymbus cavaleriei*. **H,** *Pteroceltis tatarinowii*. **I,** *Radermachera sinica*. **J,** *Triadica rotundifolia*. **K,** *Psydrax dicocca*. **L,** *Cleidion bracteosum*. **M,** *Cryptocarya calcicole*. **N,** *Cyclobalanopsis glauca*. **O,** *Ficus glaberrima*. **P,** *Glycosmis pentaphylla*. **Q,** *Litsea salicifolia*. **R**, *Micromelum integerrimum*. **S**, *Murraya paniculate*. **T**, *Myrsine kwangsiensis*. **U**, *Sinosideroxylon pedunculatum*.